



Since January 2020 Elsevier has created a COVID-19 resource centre with free information in English and Mandarin on the novel coronavirus COVID-19. The COVID-19 resource centre is hosted on Elsevier Connect, the company's public news and information website.

Elsevier hereby grants permission to make all its COVID-19-related research that is available on the COVID-19 resource centre - including this research content - immediately available in PubMed Central and other publicly funded repositories, such as the WHO COVID database with rights for unrestricted research re-use and analyses in any form or by any means with acknowledgement of the original source. These permissions are granted for free by Elsevier for as long as the COVID-19 resource centre remains active.



Contents lists available at ScienceDirect

Chaos, Solitons and Fractals

Nonlinear Science, and Nonequilibrium and Complex Phenomena

journal homepage: www.elsevier.com/locate/chaos

COVID-19 pandemic models revisited with a new proposal: Plenty of epidemiological models outcast the simple population dynamics solution

Ayan Paul^a, Selim Reja^a, Sayani Kundu^b, Sabyasachi Bhattacharya^{a,*}^a Agricultural and Ecological Research Unit, Indian Statistical Institute, Kolkata 700108, West Bengal, India^b Systems Ecology & Ecological Modelling Laboratory, Department of Zoology, Visva-Bharati University, Santiniketan 731235, West Bengal, India

ARTICLE INFO

Article history:

Received 9 November 2020

Revised 13 January 2021

Accepted 15 January 2021

Available online 19 January 2021

Keywords:

Relative growth rate

Disease fitness

Coronavirus

Steady state

Acceleration

Lockdown

ABSTRACT

We have put an effort to estimate the number of publications related to the modelling aspect of the corona pandemic through the web search with the corona associated keywords. The survey reveals that plenty of epidemiological models outcast the simple population dynamics solution. Most of the future predictions based on these epidemiological models are highly unreliable because of the complexity of the dynamical equations and the poor knowledge of realistic values of the model parameters. The incidence time series of top ten corona infected countries are erratic and sparse. But in comparison, the incidence and disease fitness relationships are uniform and concave upward in nature. These simple profiles with the acceleration curves have fundamental implications in understanding the instinctive dynamics of the corona pandemic. We propose a simple population dynamics solution based on the incidence-fitness relationship in predicting that a plateau or steady state of SARS-CoV-2 will be reached using the basic concept of geometry.

© 2021 Elsevier Ltd. All rights reserved.

1. Introduction

The coronavirus pandemic has become an unparalleled one in modern human history. Its impact has spread far and wide across the world and through all sections of the society. The severity of the disease is increasing rapidly; the World Health Organisation (WHO) is compelled to declare the pandemic of COVID-19 as a state of global emergency on 11th March 2020. So, the researchers across the globe are trying to provide their valuable insights to understand the dynamics of the coronavirus spreading. The mathematical modelling is one of the major yardsticks to be used by several authors [25,30,33,35,40,47,49,52] to portray the current epidemic/pandemic situation in several countries. Note that, most of the research work on this domain is developed based on the epidemiological models with various components. But surprisingly, the population dynamics growth models are substantially ignored, although it can compete with the existing epidemiological models. These population dynamics models are relatively simple, easy to interpret and consist of only a few numbers of parameters. The

study of Jakhar et al. (2020) [31] points out that the COVID-19 pandemic will be ended on 16th October 2020 in India, but the number of active cases on that day is 63,371. However, Ranjan (2020) [56], Tiwari et al. (2020) [70], Nadim and Chattopadhyay (2020) [45] predict that the corona infection will attain its peak on 22nd–28th April, 16th April, and in May respectively. But, the peak of the ongoing pandemic in India is observed on 17th September 2020 with the caseload 97,894. Tiwari et al. (2020) [70] also states that in India the epidemic cases will reach its equilibrium on May, 2020. Ranjan (2020) [56], Tiwari et al. (2020) [70] use the corona infection data up to 30th March 2020, but Nadim and Chattopadhyay (2020) [45] use the epidemic dataset during the time window 14th March 2020 to 19th April 2020. So, it is worthwhile to mention that most of these future predictions based on the epidemiological models are highly unreliable because of the complexity of the dynamical equations and the poor knowledge of realistic values of the model parameters.

We feel that it is necessary to provide a brief overview to the readers about the epidemiological models, which have been developed recently for understanding the COVID-19 pandemic outbreak. It would help the audience to comprehend how the epidemiological models outcast the simple population dynamics solution. Moreover, this study will be helpful to understand the limitation of the prediction associated with the corona outbreak. Mo-

* Corresponding author.

E-mail addresses: ayaninspire@gmail.com (A. Paul), selimreja06@gmail.com (S. Reja), sayanikunduofficial@gmail.com (S. Kundu), sabyasachi@isical.ac.in (S. Bhattacharya).

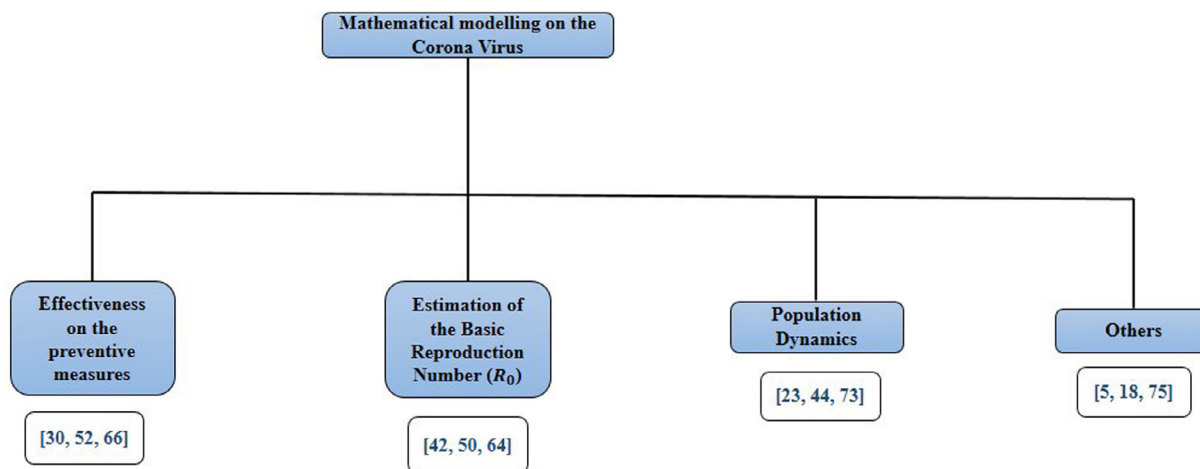


Fig. 1. Flow diagram for the mathematical modelling on the coronavirus.

hamadou et al. (2020) [43] has performed a similar kind of survey and enlisted the all possible mathematical models that have been used to understand the dynamics of COVID-19. This extensive review work can be breakdown into three major categories, such as mathematical modelling, artificial intelligence, and exploratory data analysis. This review implies that the study of the corona pandemic based on the population growth models is neglected by most of the previous authors. In our opinion, the extensive literature survey on the research work of modelling novel coronavirus can be broadly classified into four major directions viz. (i) the effectiveness of the preventive measures, (ii) the estimation of the basic reproduction number (R_0), (iii) the population dynamics solution based on the growth curve model, (iv) other concepts or frameworks excluding the epidemiological and population dynamics models (see flowchart 1). We have used the keywords *COVID*, *coronavirus*, and *corona* in the journals, publishers, and the *WHO* search engine. The total numbers of the article published on the corona outbreak both from the medical and modelling perspective are extensively large (54,236) as per the *WHO* database. We have selected four reputed publishers such as Elsevier, Springer, Nature, Science for this search. These search engines also provide information on a substantial number of publications on the corona outbreak. We have selected twelve top-rated international journals to contribute substantially to capture the recent crisis of the corona outbreak. The entire output of this web search is summarized in Table 1. We provide a column in Table 1 with the estimated percentage of the published papers that appeared in the twelve top journals on epidemiological models for exploring the corona outbreak. The 1st and 2nd point of our proposed classification actually is a part of these various epidemiological studies.

In this context, the reader may have a wrong impression of the fact that the remaining percentage of papers appeared in the journals associated with the population dynamics and the growth curve models, but this is not the fact. Most of these papers have a background with networking [18,24,74], statistical distributions [2,5,67,78], and many other mechanistic models. These all domains of research work will fall into category (iv) of our classification.

We have identified only five articles, which have a direct association with the population dynamics and the related growth curve models [4,23,48,58,72]. This research work can cover the number (iii) of our classification. The associated mathematical modelling issues are depicted through a flowchart described in Fig. 1. These findings strongly suggest that the epidemiological prediction models on the corona pandemic castaway the simple population dynamics solution. We are interested to provide a novel solution to understand the corona pandemic using the concept of population dynamics

and growth curve models. In this context, we feel that an elaborate review of the population dynamics solution on the corona pandemic is essential. We will discuss this part in the subsequent section.

Based on the number of cumulative corona infection (up to 14th September 2020) we consider the top ten countries (Fig. 2) for our further analysis. The simple graphical representations (Figs. 4a–6a) suggest that the incidence time series of top ten corona infected countries are erratic and sparse. But in comparison, the incidence-fitness relationships are uniform, and it is concave upward in nature (Figs. 4b–6b). By fitness, we mean the relative growth of the incidence of the corona disease. These simple profiles with the acceleration curves have fundamental implications in understanding the instinctive-dynamics of the corona pandemic. We will estimate the incidence-fitness profiles for these countries using the Gompertz and theta-logistic rate equations. We propose a simple population dynamics solution in predicting that a plateau or steady state of SARS-CoV-2 will be reached using the definition of three phases (lag, log, and stationary) of estimated growth curves and the basic concept of geometry. The rest of the manuscript is organized as follows. The literature review on the proposed classification and the population dynamics with the growth curve models towards the COVID-19 pandemic are presented in the Sections 2 and 3, respectively. Subsequently, we present the advantages of the relative growth rate (RGR) in the Section 4. The proposition of the novel methodology is present in the Section 5. However, the outcomes from the study and the detailed discussion are well discussed in the Sections 7 and 8, respectively. Finally, we made a conclusive statement in the Section 9.

2. Existing literature based on the proposed classification

The research in the domain of the first category of our classification is primarily based on the different prohibitive measures by several countries to stop the spread of the novel coronavirus but among those measures, the two most important paradigms are the self-isolation and the maintenance of the physical distancing. The incremental effect of these particular preventive steps is discussed by several researchers [30,50,52], etc. Singh and Adhikari (2020) [65] perform an explicit analysis on the effect of social distancing through the incorporation of the social contact structure by classifying the number of contacts made by a person into at home, workplace, school, and other contacts, etc. The basic reproduction number is thought to be a formidable measure to illustrate any epidemic situation. The estimation of the reproduction number would thus provide an important clue in understanding

Table 1

The number of research article published on the coronavirus in some reputed journals of mathematical biology from January to September 2020. The last column denotes the approximate percentage of epidemiological models published on the novel coronavirus.

Key words	Publisher	Journals	No. of articles	Percentage (approx)
-	WHO database*	-	54,236	-
-	Elsevier*	-	5099	-
-	Nature†	-	67,753	-
COVID/coronavirus		Science‡	165	-
COVID/coronavirus	Elsevier	Journal of Theoretical Biology	8	50 %
coronavirus	Elsevier	Theoretical Population Biology	1	100%
COVID/coronavirus	Elsevier	Chaos, Solitons and Fractals	260	52 %
COVID/corona	Elsevier	Applied Mathematics and computation	7	14%
COVID/corona	Elsevier	Applied Mathematical Modelling	6	50%
COVID/coronavirus	Elsevier	Mathematical Biosciences	13	77%
COVID/coronavirus	Elsevier	Journal of Mathematical Analysis and Applications	5	-
COVID/coronavirus	Springer	Bulletin of Mathematical Biology	7	43%
COVID/coronavirus	Springer	Journal of Mathematical Biology	1	100%
COVID/coronavirus	Plos One	-	3303	-
COVID/corona/coronavirus	The Royal Society ^b	-	28	14%

* Source: WHO corona Dashboard.

† Source: Nature index.

‡ Source: COVID-19 Open access.

^b Source: Official page of Science

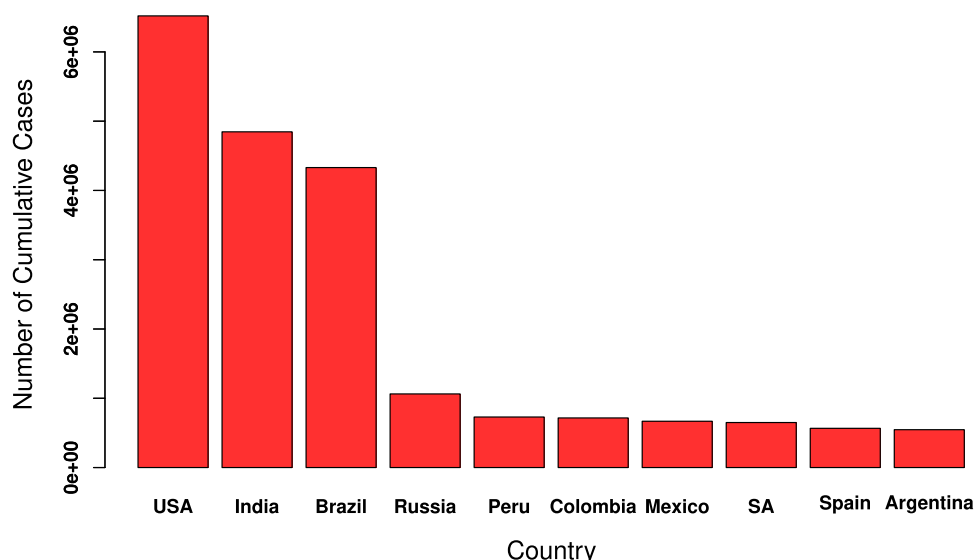


Fig. 2. The number of cumulative infected cases due to the coronavirus disease in the top ten countries as on 14th September 2020. The index SA mentioned in figure is nothing but the abbreviated form of the country name South Africa.

the spreading dynamics of any epidemic disease. So, its significant impact motivate a group of researchers to estimate the basic reproduction number for those several provinces affected with the novel coronavirus [39,42,63,77]. The study of Mizumoto and Chowell (2020) [42] point out that the magnitude of the basic reproduction number is not going to be constant throughout any fixed time domain. These studies can cover the 2nd point of our classification [42].

Kermack and McKendrick [32] initiated the epidemiological study through a seminal contribution. The author classified the population into three groups viz. susceptible, infectious, and recovered (removed). The dynamics of these group of the population is governed through the ordinary differential equation. This multidimensional model is then popularly known as the SIR model. Several epidemiological models are derived to study the corona pandemic. Susceptible-Exposed-Infected-Removed (SEIR), Susceptible-infected-recovered (SIR), Susceptible-Infectious-Quarantined-Recovered (SIQR), Susceptible-Exposed-Infectious-Quarantined-Recovered (SEIQR), Bats-Hosts-Reservoir-People transmission network (BHRP), Susceptible-Exposed-Symptomatic-Asymptomatic-Recovered-seafood

Market (SEIARW), etc. are quite a few examples of such model dynamics. The SEIR models are used for the dynamics, prediction, management strategies, effect of temperature, and humidity levels of the ongoing situation [21,29,51,54,75,76]. Similarly, track transmission and recovering rates in time, data fitting are well understood by the SIR structured models [10,17,27,38,66,68]. Both of the quarantine and management strategies are imposed through the SIQR models [20]. The prediction and management strategies have been elicited through the SIQR epidemic structure [71]. The simulation-based study on the transmission of coronavirus from the bats to humans is also explored through the BHRP like structures [16]. The age-dependent transmissibility and prediction are present in the modelling structure of SEIARW [80]. Note that, the nonconstant nature of the reproduction number of the ongoing pandemic disease depicts the brutal character of the novel coronavirus towards the human population. Zhao and Chen (2020) specified that due to the distinct characteristics of the COVID-19 from the other infectious diseases, it is hard to model the ongoing pandemic scenario through the general epidemiological structures viz. SIR, SEIR, SIQR, etc. [79]. In this connection, the author pro-

posed the *SUQC* structured model to demonstrate the dynamics of the corona infection.

3. Literature review on the population dynamics and growth curve models

The application of the population dynamics in predicting the ongoing pandemic scenario is first observed in the study of Roosa et al. (2020) [58]. The authors use the logistic growth curve, Richards law, and the recently developed sub-epidemic model [19] to forecast the ongoing pandemic situation. The cumulative number of corona infected cases (from 22nd January 2020 to 9th February 2020) of several provinces from China including Hubei have used to provide short-term (5, 10, 15 days) forecast from the base period, 9th February 2020 to onwards. The predicted figures for the number of cumulative cases on the 24th February 2020 in both Hubei and the other provinces are estimated through the range 37,415 - 38,028 and 11,588 - 13,499, respectively. The validation can be done with the observed number of cases (77,266), which is available in the [WHO corona dashboard](#). The proximity of the proposed model to the observed cases seems to be extremely poor. The observed cases are more than double the predicted cases. In another study, Wang et al. (2020) [72] use the *Fbprophet* model in addition to the logistic growth law and applied a machine learning algorithm for predicting the *Epidemic peak point*, *The fastest growth point*, *Turn point* of the corona outbreak. They use the data of the number of cumulative corona infected and the number of cumulative recovered cases in some selected countries such as Brazil, Russia, India, Peru, Indonesia, and the whole world as well. Here, the *Epidemic peak point* is defined as the time after which the number of cumulative infections will decrease. Here also, the prediction method is contemptibly poor, which can be easily verified through the [WHO](#) data.

Fokas et al. (2020) [23] use the Riccati equation for predicting the stabilizing time of this epidemic based on the data of six countries viz. Italy, Spain, France, Germany, USA, and Sweden. Note that, the logistic law with a time-dependent instantaneous growth rate (henceforth, IGR) leads to the famous Riccati equation. The author assumes that the basic characteristics of the particular virus and the cumulative effect of the variety of the different measures are taken by the given countries for the prevention of the spread of the viral infection, is time dependent. This justifies the authors' time-dependent IGR of the Riccati equation. But unfortunately, the authors are unable to explain the specific mathematical form (rational and bi-rational) of the time-dependent growth rate of Riccati equation from the epidemiological perspectives. The authors have selected these analytical expressions of time-dependent IGR by a trial and error experiment based on 50 different functional forms in a completely arbitrary manner. We feel that the way of selection of IGR is sloppy and lack of justification. Moreover, in the epidemiological study, the function should be derived phenomenologically rather than in a mechanistic way by trial and error method. The incorporation of the machine learning and associated artificial neural network and recurrent neural network is a useful extension of the Riccati equation in predicting the steady state behavior of the corona epidemic. But, this sophisticated model is also failed to meet the observed time line of the disease steady state for the considered countries. The data set provided by [WHO](#) elicits that the epidemic in those countries are yet not reached to its plateau and all the time series follow an increasing pattern. Aviv and Aharoni (2020) [4] predict the disease dies out time-line using the theta-logistic model structure based on the data of four Asian provinces such as the Chinese Mainland, Iran, the Philippines, and Chinese Taiwan, respectively. The author's prediction is also unreliable as the previous authors. He did not provide any justification

for the selection of the theta-logistic equation from a vast family of growth curve models.

Pelinovsky et al. (2020) [48] consider the growth equation approach for comprehending the dynamics of the novel coronavirus. But surprisingly, the authors have selected five countries such as Austria, Switzerland, Netherlands, Italy, Turkey, and South Korea, respectively, where the corona infection almost dies out as per the recent record. The authors frame the entire work into two aspects, the deterministic and stochastic. The authors used both the logistic and the extended logistic growth law in the deterministic study. This extended version is commonly known as the Blumberg growth law in the growth curve literature [11]. The profiles of the absolute growth rate against the size are estimated for all the five countries based on the underlying models. Here, the selection of the Blumberg equation is arbitrary and the authors did not provide any explanation for choosing such a model from a family of extended logistic equations. The absolute growth rate is used to determine the peak point of the disease outbreak and it is estimated for all the countries under both the logistic and the extended logistic setup. Unfortunately, the authors have used a *wrong expression* of the maximum absolute growth rate of the logistic law, which makes the entire study erroneous. The authors did not use the standard optimization technique such as the least square and grid-search method in estimating the predicted profiles. By varying the parameter space with a reasonable interval, the authors choose the optimum curve, which maximizes the value of R^2 . Thus, whether R^2 can be used as a model selection criterion in this case - the question persists. This informal estimation procedure does not possess any statistical property and so the significant tests of the parameter values are questionable. In the stochastic model, the Gaussian fit of r_{norm} is extremely poor and the test of normality is missing. Moreover, the mean and variance of the Gaussian distribution are also arbitrary. The good fitting does not necessarily mean that the underlying model is true for the data. So, it is not worthwhile to validate the model with the observed data sets, recently available in the [WHO dashboard](#) as the model is mathematically incorrect.

4. Why Population dynamics? - Advantages of the relative growth rate

Plenty of population growth models are available in ecology by which one can easily nurture the underlying species dynamics. The study of Carlson et al. (2018) [13] reveal that nowadays the concept of population dynamics is not just confined in ecology, but it can be also applied in many other fields. The single species population dynamics problem is generally studied either by size or RGR modelling [14,28,61]. The study of Sandland and McGilchrist (1979), White and Brisbin (1980) [60,73], reveal that the errors in the metric RGR show a lesser amount variation in respect to the errors present in the absolute growth rate. The authors show that a complex autocorrelation structure of the error variable is required for the fitting of the size models. On the contrary, a simple autocorrelated structure of the error variable is used during the RGR modelling. The authors [6,7,64,81], etc., discussed the advantage and the applications of the RGR modelling. Moreover, it is easy for any experimenter to identify the underlying growth dynamics through the RGR profile rather than the size time series.

4.1. Size-RGR relationship

Note that, the size-RGR relationship has fundamental implication in understanding the multiple demographic traits of the species [64]. So, we can conclude that *size and RGR* profiles are analogous with the phenotype and genotype characteristics of the

study of species genetics respectively. So, using RGR we can explore the innate property of the species, which is helpful to understand the fundamental mechanism of the species population dynamics. This RGR can also be interpreted as species fitness in ecology [15]. Here, the change of absolute growth rate to the initial size is interpreted as a measure of species fitness. The application of size-RGR relationship has been neglected in the existing literature of epidemiology. Obviously, in the study of disease epidemiology, the disease incidence and the disease fitness can be represented as a proxy of size and RGR respectively. If the disease fitness increases, the disease is more virulent. Naturally, it has an adverse effect on the susceptible population.

It would be worthwhile to study the relationship between the disease incidence and its fitness for understanding the inherent mechanism of the epidemic. The disease status is poorly manifested through the incidence time series (daily number of cases). The cumulative cases are more misleading as it is smoothing out the overall trend. Both of these two profiles are failed to capture the inherent mechanism of the disease status. The incident time series and the incidence–fitness relationships of the top three infected countries i.e. USA, India, and Brazil are depicted in Figs. 4b–6b. However, the incidence profile of the rest of the countries are in the supplementary file. The incidence time series are erratic and sparse, difficult to understand the inherent disease trend. But, in comparison to all the countries, **the incidence–fitness relationships are uniform and it is concave upward (convex) in nature.** These simple profiles have fundamental implications in understanding the instinctive dynamics of the corona pandemic. These issues are elaborately discussed in the Section 7.

The study of size-RGR relationship become popular in many ecological and agricultural studies [9,37,44,61]. In these studies, the authors used the empirical estimate of RGR, which is given by $\frac{\ln(x(t_2)) - \ln(x(t_1))}{t_2 - t_1}$ for a time interval (t_1, t_2) [22]. Here, $x(t)$ is the size of the population at time point t . Here, the term size is generic. It can be either abundance or any measured characteristics viz. weight, height, length, volume, biomass, etc. In the present study, we have represented $x(t)$ as the number of infected cases at the time point t . If the incidence-RGR relationship is showing a concave upward trend, it indicates that the underlying model may be either theta-logistic [57,64] or Gompertz [26]. If this relationship is linear then it suspects a logistic law may be suitable for the data. We notice that the incidence-RGR relationship for all the top ten (in terms of a Cumulative number of corona infection) countries give us a clue that the underlying model of incidence may be either theta-logistic or Gompertz. We estimate the parameters of these two growth equations in the subsequent Section 7.

4.2. Relationship of incidence and disease fitness (relative growth rate)

The pandemic of the corona disease was first reported in Wuhan, China at the end of 2019. Since then, the severity of the outbreak follows an increasing pattern worldwide. Fortunately, in some countries such as New Zealand, Denmark, Vietnam, etc. the disease is almost eradicated. But, most of the remaining countries the situation has gradually become worst and serious. The WHO declare the list of top ten countries, where the severity of the disease is at extreme based on the cumulative number of corona Infection (up to 14th September 2020). We took the data of those ten countries for our analysis. The countries are USA, India, Brazil, Russia, Peru, Colombia, Mexico, South Africa, Spain, and Argentina. In this connection, we will like to highlight that most of the previous studies in both epidemiological and population dynamics areas, the selection of countries are arbitrary or rather manipulative. The authors selected those countries where the proposed models have proximity with the given data. At the same time, the authors

neglected the countries where the time series are irregular. For example, in a recent study [4], on population dynamics the country India was neglected although, many epidemiologists declared India may be an epicentre of this pandemic. Surprisingly, the authors [36,45,46,55], etc. have selected the countries in a completely arbitrary manner.

The incidence profile of the corona infection in the topmost affected countries are not exhibiting a similar trend. For example, the time series of the *United States of America* and *Peru* are bimodal, whereas the incidence profiles are showing the exponential pattern for *India* and *Argentina*. The time series profiles of *Colombia*, *South Africa*, and *Mexico* are negatively skewed. The peakedness of *Colombia* and *South Africa* are high but it is low in the case of *Mexico*. The trend of *Russia* is uni-modal with high peakedness. The country *Brazil* has an erratic and sparse growth profile although, the overall trend is primarily increasing and then decreasing. *The most surprising thing is that the incidence-RGR profiles of all the top ten countries are exhibiting a monotonic decreasing trend (mostly concave upward except one).* This phenomenon is synergistic with the species growth dynamics study in the field of ecology [8,64]. Sibly et al. (2005) [64] conclude that most of the size-RGR relationships are concave upwards (convex) in nature for the species of all taxonomic groups except the large mammals although, their time series are displaying an erratic pattern. Bhowmick and Bhattacharya (2014) [8] depict that although the size profile of a fish is following an increasing trend, the RGR profile is delineating a bell-shaped structure. This structure suggests that RGR is relatively strong metric in understanding the inherent growth mechanism of the population.

4.3. Research question and mathematical challenge

Now, we have two fundamental research questions to be answered. The epidemiologists are interested in predicting the time that a plateau/steady state of SARS-CoV-2 will be reached, as well as the number of individual cases to be reported infected at that time. Here, the plateau is achieved when the RGR or the fitness of the disease is zero. Theoretically, the theta-logistic model will be reached at a steady state when the population is at the asymptotic size. Mathematically this asymptotic size will be attained when the time is infinite. It may be an interesting mathematical exercise to deal with an infinite time sequence, but in reality, while playing with incidence data of disease, it is virtually meaningless. One cannot wait up to the infinite time for a disease to be stabilized. The mathematical challenge of the problem will initiate from this issue. We know that the three broad phases of the population growth curves are the lag, log, and stationary. Unfortunately, there is no thumb rule that when the population will initiate its journey for approaching the steady state. Similarly, can we define with clarity that when the log phase of the population will be terminated? There may be some time lag between the log phase ending time (LOET) and the stationary state initiating time (see Table 2). This

Table 2
Abbreviations to be used throughout the manuscript.

Abbreviated form	Implication
RGR	Relative Growth Rate
LAET	Lag Phase Ending Time Point
LAES	Lag Phase Ending Size
SIP	Size at Point of inflexion
LOET	Log Phase Ending Time Point
LOES	Log Phase Ending Size
SSIT	Steady State Initiation Time Point
SSIS	Steady State Initiation Size
PAR	Population-Acceleration Relationship
ADITW	Average Daily Incidence of Last Two Weeks

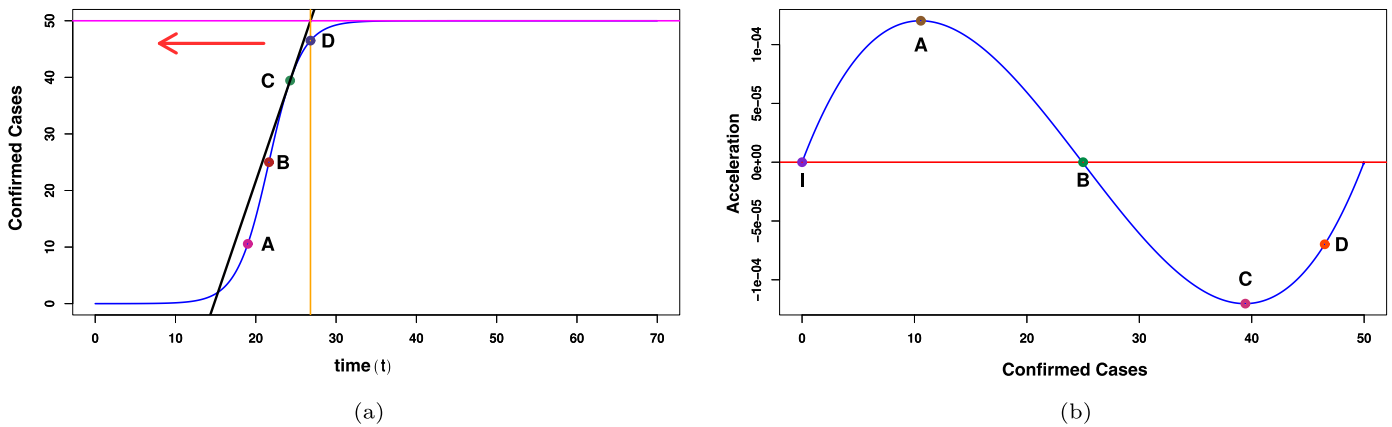


Fig. 3. Both the figures (a) and (b) denote the theoretical size and acceleration profiles of any standard sigmoidal growth trajectory respectively. The term size denotes the number of confirmed cases of corona incidence. In both the figures, the points A, B, C indicate the lag phase ending point, point of inflexion, the log phase ending point respectively. We propose the intersecting point of the vertical (orange) line with the sigmoidal (blue) curve i.e., D as the steady state initiation point of that growth curve. Moreover, the point I in the acceleration profile indicates the initial infection size. However, it is clearly ensured from the acceleration profile that the growth acceleration is maximized at the point A, minimized at the point C and vanishes at the point I, B, respectively. (For interpretation of the references to color in this figure legend, the reader is referred to the web version of this article.)

intermediate phase can be defined as the preparatory mode of the population from the log to the stationary phase transition. Similarly, there may be an intermediate phase between the lag phase ending time (LAET) and the Point of inflexion. Let us define, the size of the population at SSIT as SSIS i.e. steady state initiation size. We propose a novel methodology to estimate LOET, SSIT, and SSIS for both the Gompertz and the theta-logistic law. Finally, we have used these estimates for predicting the time and population size at a steady state of SARS-CoV-2 infection. The proposed definitions are also interpreted from the size-acceleration curves. This size-acceleration profile is helpful to compare the steady state of different countries. The concept and definition of the proposed methodology are described in the subsequent section.

5. Proposed methodology

We consider two fundamental growth equations, Gompertz and logistic, for modelling the corona pandemic data of incidence of top ten countries. The monotonic decreasing concave upward pattern of the size-RGR profile motivates us to select these two models. We elaborately discussed this issue in the preceding section. The RGR equation of the theta-logistic growth and the Gompertz curves are given by

$$\frac{1}{x(t)} \frac{dx(t)}{dt} = r \left(1 - \left(\frac{x(t)}{K} \right)^\theta \right), \tag{5.1}$$

$$\frac{1}{x(t)} \frac{dx(t)}{dt} = r \log \left(\frac{K}{x(t)} \right). \tag{5.2}$$

We assume $x(t) (> 0)$ be the corona incidence at any time point t for any specific country. The instantaneous incidence rate and the asymptotic size of the corona incidence are denoted by r and K respectively. Here, θ is the density regulation parameter, heavily dependent on the herd immunity status, personal protection, social distancing, and Government policy of the country. Now, our theoretical interest is to predict the time of a plateau of Covid incidence profile for all the top ten countries. More specifically, we have to estimate the SSITs of all the countries. Note that, this theoretical derivation of SSIT involves LOET. LAET's do not have any role in deriving the expression of SSIT. For the better understandability of the reader, we would like to provide a clear definition of LOET and SSIT. Before stating the definition, we need to familiar with the size-acceleration curve as a prerequisite theoretical

knowledge. The population time series and the size-acceleration curves are demonstrated in Fig. 3.

It is necessary to compare the movement of the population through a growth trajectory with the motion of a particle in Newtonian mechanics for a better understanding of the size and size-acceleration profile. The change of population to time is equivalent to the displacement of a particle with time. Note that, the absolute growth rate of a population is analogous with the velocity of a particle moving on a fixed path. The selection of trajectory is determined on the velocity and acceleration terms acting on the particle. Similarly, in the context of the population dynamics problem, the lengths and positions of the lag, log, and stationary phases are dependent on its velocity, and acceleration profile. By velocity and acceleration profiles, we mean two relationships viz. population-velocity and population-acceleration respectively. Essentially, there exist similar relationships viz. displacement-velocity and displacement-acceleration in mechanics. In the entire study, we will mostly focus on these relationships from the population dynamics viewpoint.

The second population-acceleration relationship (henceforth, PAR) has immense importance as it explains the internal growth mechanism of the population, which is manifested as a growth trait through the population time series. A similar concept is also introduced by Buchanan and Cygnarowicz (1990) [12] for the time-acceleration framework. We already mentioned that the size-RGR relationship has a similar property, which can explain the inherent mechanism of the population and fundamental implications in determining several demographic traits. By analyzing PAR, we observe that the acceleration vanishes for three population sizes for any sigmoidal growth equation. First obviously at the initial population size, then at the Point of inflexion, and finally at the steady state i.e., when the population attains plateau. The two most important points of this acceleration curve are the points where the acceleration attains its maximum and minimum values (Retardation is maximum). The population kicks up and enters into the log phase (see the point A in Fig. 3b) while the acceleration is maximized. Beyond this point, the acceleration gradually decreases up to the Point of inflexion (the point B in Fig. 3b). Then immediately, the population exposed to retardation (negative acceleration) and it is gradually attained its maximum at the point C (Fig. 3b). Now there is a turn to comeback the magnitude of retardation at stage zero. This is the most essential stage without which, the population cannot be reached a steady state. This maximum retardation

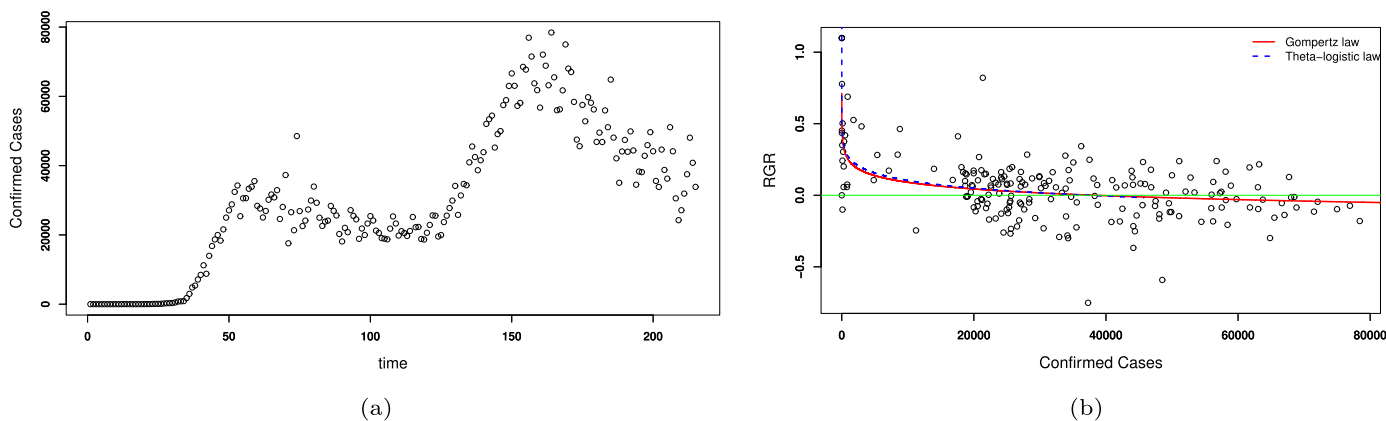


Fig. 4. The number of active corona cases of **United States of America** is projected in this figure. Here figure (a) denotes the time-series diagram and that of (b) denotes the RGR of the active corona cases with respect to the number of daily infection. Moreover, in figure (b) the RGR data is fitted against both the theta-logistic and the Gompertz Model. The fitted diagram is mentioned in the legend of figure (b).

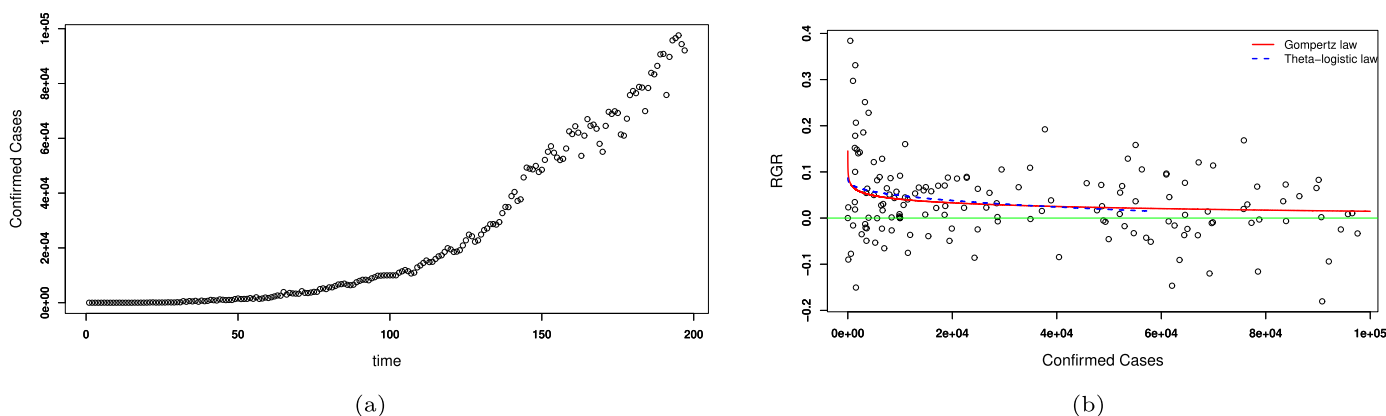


Fig. 5. The number of active corona cases of **India** is projected in this figure. Here, figure (a) denotes the time-series diagram and that of (b) denotes the RGR of the active corona cases with respect to the number of daily infection. Moreover, in figure (b) the RGR data is fitted against both the theta-logistic and the Gompertz Model. The fitted diagram is mentioned in the legend of figure (b).

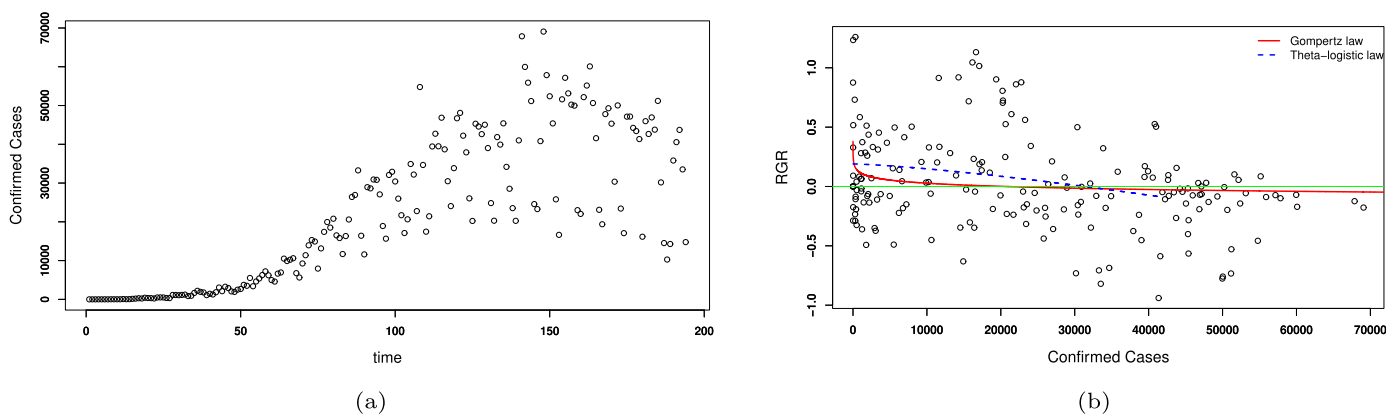


Fig. 6. The number of active corona cases of **Brazil** is projected in this figure. Here, figure (a) denotes the time-series diagram and that of (b) denotes the RGR of the active corona cases with respect to the number of daily infection. Moreover, in figure (b) the RGR data is fitted against both the theta-logistic and the Gompertz Model. The fitted diagram is mentioned in the legend of figure (b).

point can be defined as a precursor of the steady state. This is the point from which the preparation of reaching a steady state is resumed. The points *A*, *C*, *D* are abbreviated as *LAET*, *LOET*, and *SSIT* as described earlier.

Definition: A tangent is drawn at the point *LOET* on any population sigmoidal growth curves in such a way that it would certainly meet at a point with the extended (see the arrow in Fig. 3a) part of the asymptotic size (carrying capacity). Now, the projection of

that meeting point on the growth curve cuts the time axis at the steady state initiation time point.

Remark 1: We feel that the point *SSIT* has massive importance in the study of epidemiology. Here, we can assume the daily incidence disease as a population. If the daily incidence is attained *SSIS* for a fixed value of *SSIT* then we conclude that the disease under consideration is already at the preparatory stage of steady state. The estimated values of *SSIT* and *SSIS* are helpful hence to

determine the Government policy and the management actions for controlling the disease epidemic.

The theoretical formulation of *SSIT* is well explained in a flowchart depicted in the supplementary file. We need to first derive the theoretical expressions of the acceleration term and its extremum under theta-logistic and the Gompertz set up as a first step of the flowchart. We describe these expressions in the [Theorems 5.1, 5.2, 5.3, and 5.4](#).

Theorem 5.1. *The growth acceleration (a(t)) in describing the theta-logistic growth trait should be maximized when the number of infected case reaches at $x(t) = K \left(\frac{(\theta+2)(\theta+1) - \sqrt{(\theta+2)^2(\theta+1)^2 - 4(\theta+1)(2\theta+1)}}{2(\theta+1)(2\theta+1)} \right)^{1/\theta}$ and that of minimized at $x(t) = K \left(\frac{(\theta+2)(\theta+1) + \sqrt{(\theta+2)^2(\theta+1)^2 - 4(\theta+1)(2\theta+1)}}{2(\theta+1)(2\theta+1)} \right)^{1/\theta}$ respectively.*

Proof. The proof is given in the supplementary file. □

Theorem 5.2. *The growth acceleration (a(t)) in describing the Gompertz law should be maximized when the number of infected case reaches at $x(t) = Ke^{-\left(\frac{3+\sqrt{5}}{2}\right)}$ and that of minimized at $x(t) = Ke^{-\left(\frac{3-\sqrt{5}}{2}\right)}$ respectively.*

Proof. The proof is given in the supplementary file. □

Theorem 5.3. *The onset of the steady state in the theta logistic growth trajectory is observed at the time $SSIT = LOET +$*

$$\frac{1 - \left(\frac{(\theta+2)(\theta+1) + \sqrt{(\theta+2)^2(\theta+1)^2 - 4(\theta+1)(2\theta+1)}}{2(\theta+1)(2\theta+1)} \right)^{1/\theta}}{r \left(\frac{(\theta+2)(\theta+1) + \sqrt{(\theta+2)^2(\theta+1)^2 - 4(\theta+1)(2\theta+1)}}{2(\theta+1)(2\theta+1)} \right)^{1/\theta}}, \text{ where the expression}$$

$$\left(1 - \frac{(\theta+2)(\theta+1) + \sqrt{(\theta+2)^2(\theta+1)^2 - 4(\theta+1)(2\theta+1)}}{2(\theta+1)(2\theta+1)} \right)$$

of *LOET* is given by $-\frac{1}{\theta r} \log \left[\frac{\frac{2(\theta+1)(2\theta+1)}{(\theta+2)(\theta+1) + \sqrt{(\theta+2)^2(\theta+1)^2 - 4(\theta+1)(2\theta+1)}} - 1}{\left(\frac{K}{x_0} \right)^\theta - 1} \right]$

Proof. The proof is given in the supplementary file. □

Theorem 5.4. *The onset of the steady state in the Gompertz growth law is observed at the time $SSIT = LOET + \frac{1 - e^{-\frac{3-\sqrt{5}}{2}}}{re^{-\frac{3-\sqrt{5}}{2}} \left(\frac{3-\sqrt{5}}{2} \right)}$, where the*

expression of $LOET$ is given by $-\frac{1}{r} \log \left(\frac{K}{x_0} \right) \log \left(\frac{1}{\log \left(\frac{K}{x_0} \right) \left(\frac{3-\sqrt{5}}{2} \right)} \right)$.

Proof. The proof is given in the supplementary file. □

6. The data

We have selected the top ten countries based on the cumulative number of corona infections up to 14th September 2020 available on the [WHO dashboard](#). The data of the same countries are also available in the *R* package with library function *coronavirus* [34]. But the data available in *R* package is updated up to the time line June 2020. We verified the correctness of the data available from these two sources up to the overlapping time period (i.e., from the onset of the corona pandemic to June 2020) and for the remaining time window (July to September 2020), we use the [WHO](#) data only. We have cleaned the data by standard statistical techniques. This cleaning is done in such a way so that we can discard a little amount of data and avoid over-fitting. Raw data are available in the format of daily incidence for all the top ten countries. All the data are scanned and imported in the *R* environment.

7. Results

In this section, we will evaluate the estimated values of the *SSIT* and *SSIS* for the top ten countries along with an elaborate discussion of the estimation procedure. We took the help of [Theorems 5.1 to 5.4](#) for this estimation. We have estimated the model parameters for (5.1) and (5.2) using the non-linear regression analysis. For the response variable, we use the empirical estimate of RGR for disease fitness [22], which is already discussed in [Section 4.1](#). The entire statistical analysis has been performed in the *R* software [53]. We use the Gauss-Newton type algorithm for the estimation purpose [62]. The algorithm is implemented in the routine “nls” in *R* software. Note that, the non-linear least square regression procedure is highly sensitive to the initial choice of parameter values. We consider the magnitudes of the disease fitness at a very low incidence and the high incidence as the initial guess of the model parameters *r* and *K* respectively. However, the convergence of the least square process on the theta-logistic law is sometimes uncertain due to the presence of non-linearity in that model 5.1. One should opt for the grid search process to choose the initial guess to avoid the divergence of the least square technique. Several authors used the concept of grid search in their articles for the estimation purpose [9,59].

Initially, we provide a range of values of the parameter θ for each of the ten cases to start the grid search process. The linear regression technique of RGR on x^θ and $x^{\theta+1}$ (with no intercept term) is then performed by considering all of these predefined values. The linear regression is used through the routine “lm” in *R* software [53]. We consider the best grid estimate of θ ($\hat{\theta}$) based on the lower residual sum of squares (RSS). The result of the linear regression also provides the estimates of the parameters *r* and *K*. Bhowmick et al. (2015) [9] mentioned that the grid estimates may sometimes produce bias and may not be consistent with the corresponding growth equations. To get the more precise estimates of *r* we perform the bootstrap linear regression method of RGR on $x^{\hat{\theta}}(t)$ and $x^{\hat{\theta}+1}(t)$, where the parameter θ is substituted by that grid estimate $\hat{\theta}$. The process is replicated for 10000 times to find the distribution of the parameter *r*. We treat the mean of that distribution as the final estimate of the corresponding model parameter *r* (\hat{r}). The generated \hat{r} has now plugged in the theta-logistic model (5.1) to find the consistent estimate of the two other model parameters *K* and θ respectively. It is needless to say that we use the grid estimates of θ and the estimated values of *K* in the above linear regression as the initial guess in the non-linear regression technique. Due to the reduction of the number of parameters and the choosing of the proper initial guesses, the convergence of the *nls* process has become certain and we get \hat{K} and $\hat{\theta}$ respectively.

We perform the model selection based on the Akaike Information Criterion (AIC) [1]. The lower value of AIC is used to select a better model. The estimated model parameters for all the ten mentioned countries along with the AIC values are listed in the corresponding tables. Tables are presented in the supplementary file. A summarised version of table is available in the subsequent [Section 8](#). We use these estimated values of the model parameters for our further analysis. We plug the estimated values of the model parameters in the expression of *LOET* and *SSIT* as available in the [Theorems 5.1 to 5.4](#). We also enumerate the *SSIS* for all countries based on the *SSIT* estimates. These estimates are depicted in [Table 3](#).

8. Discussion

The effect of the novel coronavirus on the human population is creating a scary situation day by day. Throughout the globe, the infection number is increasing by leaps and bounds. Scientists are exploring many avenues in predicting the time and size

Table 3

The calendar date and the attainment time with size of the steady state initiation of the confirmed COVID cases for the top ten countries. The predicted calendar time are based on the data up to 14th September 2020. Note that, the column *Average daily incidence* and *Total population size* represent the last two weeks average number of incidence due to the corona pandemic and the demographic population size of the corresponding countries respectively.

Sl. No.	Country	SSIT	SSIS	Date	Average daily incidence (two weeks)	Total population Size
1	USA	63.21 days	33363.49	16/11/2020	37226.47 ± 2015.92	331,420,450
2	India	38.35 days	87632.63	22/10/2020	86912.93 ± 2237.52	1,382,900,689
3	Brazil	63.89 days	29359.28	16/11/2020	32286.8 ± 3851.59	212,883,816
4	Russia	47.2 days	6555.37	31/10/2020	5493.73 ± 380.65	145,948,080
5	Peru	37.86 days	4224.99	21/10/2020	6012.26 ± 399.64	33,069,039
6	Colombia	120.56 days	6681.67	12/01/2021	7760.33 ± 250.98	50,998,462
7	Mexico	89.75 days	3689.18	12/12/2020	5111.26 ± 255.90	129,221,511
8	South Africa	84.01 days	5908.4	07/12/2020	1816.13 ± 128.18	59,467,369
9	Spain	187.84 days	32506.3	20/03/2021	12018.13 ± 1622.13	46,758,719
10	Argentina	89.33 days	5888.302	25/12/2020	10297.27 ± 444.88	45,284,429

of the steady state population of daily incidence for the disease SARS-CoV-2 will be reached for different countries. For this purpose, we propose the two concepts viz. *SSIT* and *SSIS*, which we already discussed in the previous section. Actually, as per this concept, *SSIS* can be interpreted as a corridor for reaching the steady state of a disease. In other words, the preparatory stage for reaching the steady state is going to initiate if a country will attain its *SSIS* value. The magnitude of *SSIT* and *SSIS* will depend mostly on the population-acceleration relationship (*PAR*) of the disease incidence for all the countries, which we will discuss in the subsequent paragraph of this section. Before this, we feel that it is important to discuss the relative performance of the disease status based on the *SSIT* and *SSIS* values of different countries. For this purpose, we introduce an additional column in [Table 3](#) along with the *SSIT* and *SSIS*, where the average daily incidence (with standard error) of the last two weeks (henceforth, *ADITW*) is represented for all the countries. The *ADITW* and *SSIS* are more or less compatible with the top seven countries. The top five countries will be entered into the steady state or in other words, the corona status of these countries will be loitering around its steady state corridor within October (or next two months). The standard error and the daily incidence are not significantly high for most of the countries. Brazil and Spain have relatively high standard error in comparison with their *ADITW* values. As per our prediction, the chance of steady state initiation is not before the end of December 2020 or January 2021 for the countries Colombia, Mexico, South Africa, Spain, Argentina. Note that, the *ADITW* values for South Africa and Spain are far away from the predicted *SSIS* values. These imply that there is a chance of increasing the expected daily incidence for the two countries South Africa and Spain, within the upcoming four months period from the calendar date 14th September 2020. The performance of our prediction model is not satisfactory for the country Argentina. We observe that in the case of Argentina, the fitness of the disease COVID-19 is exhibiting either low or high values for the low incidence - this is no doubt an unrealistic phenomenon from the concept of epidemiology. The data impurities may be the prime factor for this anomaly.

Remark 2: In this connection, it is worth sharing an important statement with our readers about the prediction models and its illustration with the real data in the existing pieces of literature. In most of the recent studies, the authors have selectively chosen the data of different countries for the illustration so that they can efficiently show their model performance very easily [36,45,55]. We believe this is a sort of manipulation for showing the proximity of the data to the proposed model. We have not chosen the data arbitrarily. We have selected the top ten countries based on the severity of the cumulative incidence data. We deliberately not discarded the prediction procedure for the country Argentina even the model performance is poor and not satisfactory.

Table 4

Estimated model parameters for the daily incidence data sets of the corona disease in the top ten countries. The detail analysis of the model parameters for each of the countries is presented in the supplementary file.

Sl. No.	Country	\hat{r}	\hat{K}	$\hat{\theta}$
1	United States of America	1.53	37237.27	0.05
2	India	0.167	97668.91	0.14
3	Brazil	0.19	31333.1	1.34
4	Russia	0.54	7247.7	0.22
5	Peru	0.54	4638.7	0.37
6	Colombia	0.15	7297.45	0.5
7	Mexico	51.4	4130.32	0.001
8	South Africa	55.4	6614.88	0.001
9	Spain	25.7	36393.1	0.001
10	Argentina	52.1	6592.4	0.001

8.1. Comparison of *SSIS* values of top three countries

If we compare the *SSIS* values with the steady state estimate available in [Table 4](#), we observe that both are compatible and realistic. We need to take the help of *PAR* analysis for identifying the inherent cause with varying *SSIT* and *SSIS* values. For this analysis, we choose the top three countries having maximum cumulative incidence cases. We have already mentioned that these three countries have similarities in connection with the current status of the corona pandemic. The *ADITW* values are pretty close with the predicted *SSIS* values from the model. From the velocity population profile, we observe that the size at the point of inflexion (henceforth, *SPI*) for India is high in comparing two other countries USA and Brazil. The *SPI* is almost the same for USA and Brazil ($p - value > 0.05$). The variance of the expression *SPI* are obtained by the univariate delta method. The detailed testing procedure is present in the supplementary file.

The general structure ([Fig. 3b](#)) of *PAR* has been reflected in the output of the incidence-acceleration profile ([Fig. 8b](#)) of these three countries. Note that, there is a significant variation among the acceleration trajectories. The incidence values for which the acceleration will attain the peak, the retardation will be maximized or acceleration will be returned to zero are the three yardsticks for explaining the internal mechanism of the corona epidemics. The rate and magnitude of the acceleration of corona incidence will depend on the Government policy and social awareness (i.e., social distancing, masking, sanitization), immunity states of population, and virulence of the viral strain. For this reason, the rate of change in accelerations and its peak values are higher for Brazil and USA in comparison with India. Existing studies reveal that the immunity status of the Indian populations is comparatively better in comparison with the other two countries. Similarly, the virulence of the viral strain is also weak in the case of India. It is worth men-

Table 5

The estimated magnitudes of LAES, SPI, LOES, and SSIS for the countries USA, India, and Brazil, respectively.

Sl. No.	Country	LAES	SPI	LOES	SSIS
1	USA	3020.728	14034.34	25716.05	33363.49
2	India	9330.494	38308.32	68763.72	87967.67
3	Brazil	7761.194	16613.81	25367.02	29359.28

tioning that community transmission has not yet been initiated in India according to WHO. They claimed that a cluster of cases has observed in the Republic of India (WHO corona dashboard). We believe, this should be the reason, why the incidence-acceleration profile of India is exhibiting a slow rate of the upward and downward movement. WHO also mentioned that community transmissions were detected in the two countries USA and Brazil, before a reasonable number of period, and this leads the incidence-acceleration profile for Brazil to show up a sharp rate of increase with a high peak value. A moderate peak value is identified in the acceleration profile of the USA, but the rate of acceleration is pretty high. For the USA, the peak of acceleration is observed for the lowest incidence value of 3020.73. So, the corona outbreak kicks up, and a sharp log phase initiates (LAES) when the country is exposed only to the low number of corona incidence (Fig. 8b). The incidence at that Point of inflexion (SPI) is 14034.34. This LAES and SIP values are respectively 7761.194 and 16613.81 for Brazil, which is slightly higher than the USA. These estimates are 9330.49 and 38308.32 for India. Both are pretty high in comparison with the other two countries. So, the corona caseload for India provides a jerk at a reasonably high incidence value, and the log phase starts. The acceleration of the incidence will be zero at SPI, and the retardation initiates for India. The retardation will be maximized, with a slow rate and the log phase ends with the incidence value of 68763.72. Moreover, the preparation of steady state starts with an incidence value of 87967.67 (SSIS) at SSIT. Note that, the population in India is the largest among the top three countries. This large population may be one of the reasons that for India the infection has spread out in pockets and clusters. Moreover, the relatively stronger immunity of the people and the weak virulence of the disease lead to a low peak of the acceleration curve. So, in a nutshell, the outbreak of the corona disease status for India will be a plateau with very high daily incidence cases but with a low spreading rate (Table 5).

8.2. Analysis of lockdown and unlock phases of India

The first case of the corona was identified in India on 31st January 2020. The caseload was restricted on an average of ten daily incidences up to the end of the March 2020. But at the end of March 2020, there was a substantial spike in daily incidence cases, and the India corona status suddenly became severe. As preparation for lockdown, the Government of India announced a “JANTA CURFEW” for intimating the general people of India on corona severity and need to break the chain of the high rate of infection on 22nd March 2020 (News on “JANTA CURFEW”). Then immediately, the first complete lockdown schedule (25th March-14th April 2020) has been announced. Based on the severity and the aggressive nature of the disease the Government of India extended the first lockdown in additional three phases. There were several attempts by the Indian Government to unlock the lockdown status in three phases viz. Unlock 1.0, Unlock 2.0, and Unlock 3.0 up to the calendar time 14th September 2020. The timelines for four lockdowns and three Unlock phases are enlisted in Table 6. There was an expectation from the Government of India that the extension of lockdown in four uninterrupted phases should have a direct impact on the variation of steady state attainment time. This

implies the estimated values of the proposed SSIT measure should be changed dynamically with the lockdown phases. We have estimated the SSITs at the end of all the four phases of lockdowns and three additional unlock phases. We should expect that the lockdowns can break up the chain of the severity of the incidence, and as a result, the SSIT values may be decreased at the end of all lockdowns. But surprisingly, we notice that the percentage increase (120%) in the magnitude of SSIT is maximized when the population is moved from the end of the second to the third lockdown. This significant increase may be due to introducing the special trains for shifting the migrant workers from one state to another without proper planning. The percentage of increment is pretty low (24.22%) in between the third and fourth phase lockdown. The percentage is decreased when the migratory workers are settled down in their home town and the Government takes immediate precaution for maintaining the social distance and other personal protection measures. The evaluated percentage increase in the SSIT value at the end of the second phase of lockdown is 63.05%. This percentage increase is more or less equal (69.91%) between the fourth lockdown and Unlock 1.0. This increased percentage in comparison with the third and fourth phase lockdown is may be due to the Government announcement on relaxing the social activities of the general people. Surprisingly, when the population completed the Unlock 3.0 phase from Unlock 2.0, the SSIT value was decreased which means the Unlock 3.0 phase does not have any significant impact on changing the SSIT values on completion of the Unlock 2.0 phase. This is no doubt a strong indication that India is going to attain a steady state shortly. In a nutshell, we can conclude that the proposed SSIT measure can capture the overall corona status of the country in a very clear and comprehensive way.

8.3. Possibility of eradication: a clue from the model

In epidemiology, elimination of a disease from a specific area (zero cases) is termed as ‘eradication’; while pocketed and sometimes unstable elimination of the disease is called as ‘under control’ [3]. Proper eradication of COVID-19 is only possible through successful vaccinations to the entire human population. Several countries all over the world are trying to discover vaccine to get rid of the SARS-CoV-2 infections (coronavirus vaccine development) Among such endeavors, Oxford University with the collaboration of the AstraZeneca, UK, and Gamaleya Scientific Research Institute of Epidemiology and Microbiology, Moscow, Russia (Russia news) are running forward this race. The clinical trials of vaccine discovery by both the organizations are in between the human trial phases III and IV. Though, no such full proved vaccine is yet developed for the coronavirus, so we can not say surely whether the eradication of this disease will be possible or not. But we can hope that in the long run, this disease also can be controlled or eradicated like the previously mentioned global epidemic/pandemic diseases, if successful vaccines are discovered [41].

In the present study, the disease elimination process starts when the hypothetical time series of incidence will attain its asymptotic size. We can think of the generation process of this hypothetical elimination/eradication trajectory in a very simple way. For this, we have to assume the SSIS estimate as the initial value of the eradication process. Note that, the incidence value will be reached at zero if the disease will attain its eradication state. Disease control may be an alternative of eradication, if we allow a relaxation in terms of minimum population size. In the case of disease control, we can assume a minimum population size (not zero) so that the theoretical existence of the theta-logistic model is preserved. This minimum population size is the estimate of the carrying capacity of the eradication curve. It is worthwhile to mention that the incidence and eradication profiles should be generated from the same underlying model. Apart from the initial and

Table 6

The dynamical change of the steady state reaching time due to different phases of lockdown in India as on 25th March 2020. The fourth column *SSIT* indicates the steady state initiation time point. The dates of the lockdown/Unlock phase are declared by the Government of India. The last column denotes the change in the percentage of *SSIT*'s between the consecutive lockdown and Unlock phases in India.

Sl. No.	Lockdown / Unlock	Duration of Lockdown / Unlock Phase	SSIT	Date	Percentage Increase
1	First Lockdown	25/03/2020 - 14/04/2020	21.33 days	15/04/2020	-
2	Second Lockdown	15/04/2020 - 03/05/2020	34.78 days	28/04/2020	63.05
3	Third Lockdown	04/05/2020 - 17/05/2020	76.58 days	09/06/2020	120.18
4	Fourth Lockdown	18/05/2020 - 31/05/2020	95.13 days	28/06/2020	24.22
5	Unlock 1.0	01/06/2020 - 30/06/2020	161.64 days	02/09/2020	69.91
6	Unlock 2.0	01/07/2020 - 31/07/2020	246.88 days	26/11/2020	52.73
7	Unlock 3.0	01/08/2020 - 31/08/2020	233.3 days	13/11/2020	-5.5

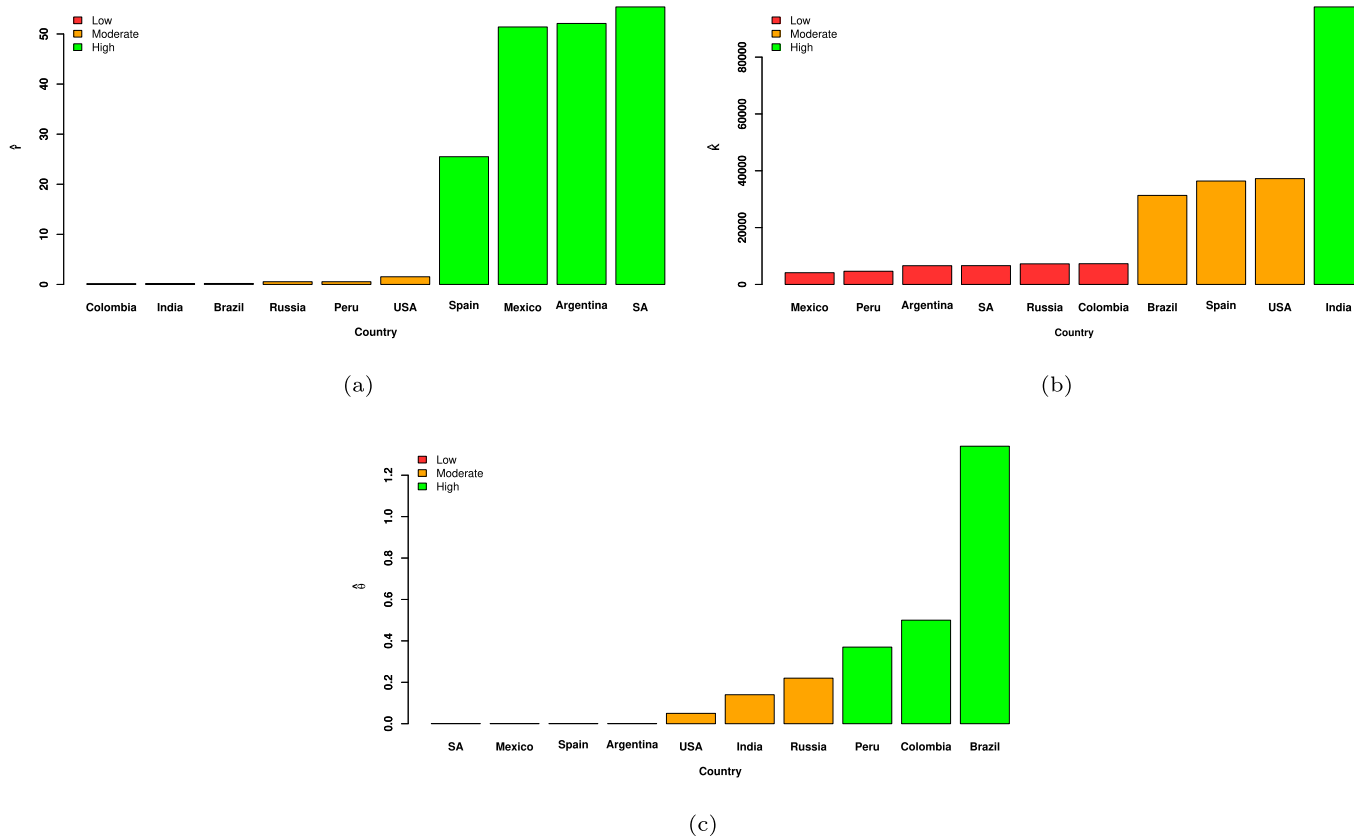


Fig. 7. Bar diagram of the estimated model parameters involved in the theta-logistic model 5.1 according to the ascending order.

the asymptotic size, we need an estimate of the intrinsic growth rate for the generation of the eradication curve. This intrinsic rate of the eradication process should be the convolution of the three processes viz. (i) the rate of the production of the vaccine; (ii) the implementation time of the vaccine, and (iii) the rate of immunity gain on the application of the vaccine. To describe all of these three above mentioned points, we have to go through a rigorous literature review on the global epidemiology and recent news releases by the different national or international officials. We have to establish a relationship among these three criteria by searching step-by-step information from the news updates, literature, and previously occurred epidemic/pandemic diseases case study reports like Tebbens et al. (2010) [69], did for his work. The present study is mainly focused on predicting the time of getting 'under control stable status' with a specific number of active cases of COVID-19 for the Indian population, only by using the world epidemic/pandemic, eradicated/non-eradicated diseases, and the vaccination data. Henceforth, we can define it as the eradication rate.

The prediction procedures start with the determination of the probable minimum population size of COVID-19 infections in India

in the long run. A case study on polio epidemics shows that the number of the world annual paralytic polio cases reduced to 43 in 2016 from the incidences of 450,000 in 1981. As of 2019, it is almost eradicated from different parts of the world, but only in three countries: (Afghanistan, Nigeria, and Pakistan) wild poliovirus is still endemic ([Global news on the eradication of disease](#)). Another case study on the Murine Typhus disease in the United States informs that the lowest number of total annual reported cases was 47 at the time of local elimination of the disease [3]. The author mentioned that the case number may vary from one study to another. He took the number 50 as the lowest Murine Typhus infected person for further analysis. In the spirit of these explanation, we assume that the probable minimum number of annual COVID infection in the long run to be 50.

The next approach is to determine the rate of vaccine production for India. The Serum Institute of India, Bharat Biotech and many others are working on the COVID-19 vaccines in India ([Report on vaccine production in India](#)). News release of the Serum Institute of India claims on 28th May 2020 that 1 billion doses of vaccines could be supplied

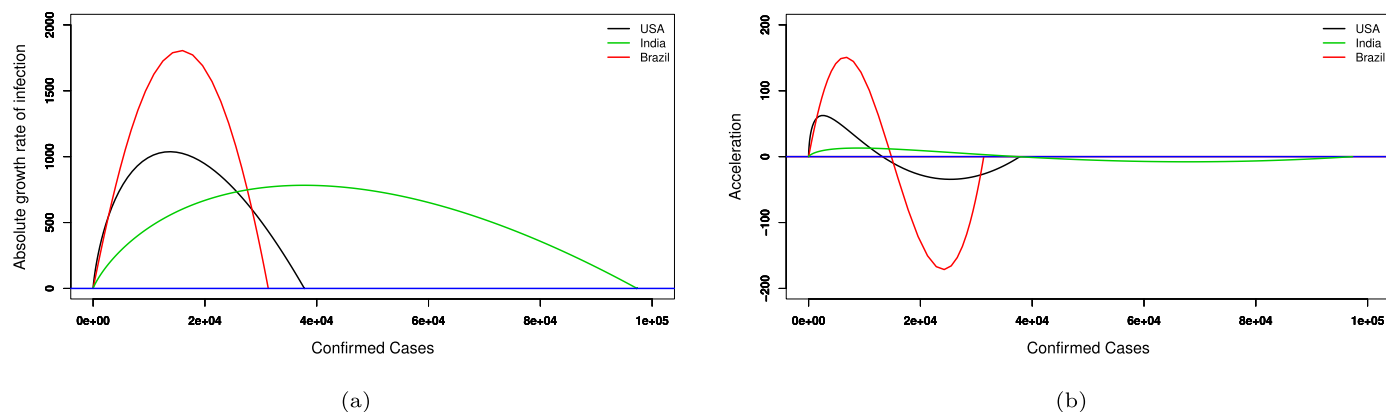


Fig. 8. Figure (a), (b) describe the estimated absolute growth velocity (AGR) and the estimated growth acceleration profiles, concerning the number of corona infected cases in the top three affected countries respectively.

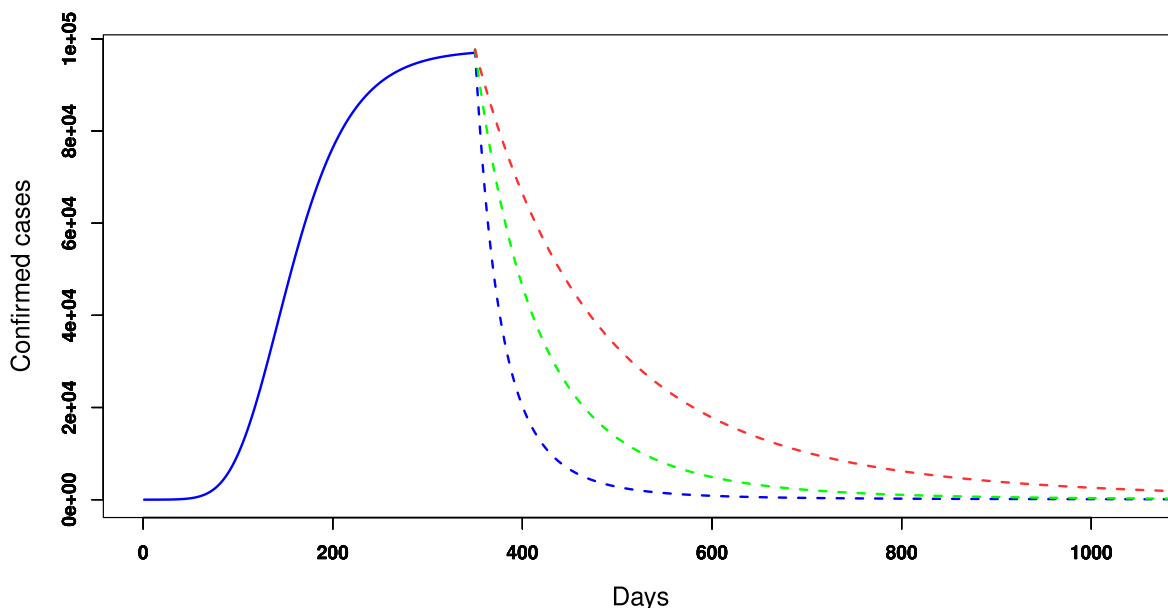


Fig. 9. The curves represent the hypothetical predicted time series of the disease incidence profile for India. The solid (blue) line is due to the increment in the disease incidence with the rate $r = 0.167$. The magnitudes of the others parameters to be used for the (solid blue coloured) profile $K = 97668.91$, $\theta = 0.14$. The dashed lines are the hypothetical disease eradication profile. We consider $r = 0.019, 0.004, 0.002$ for the blue, green, red dashed line respectively. We choose the theta-logistic growth law as the underlying model for both the incidence and the eradication profile. In case of the eradication profile, we use $K = 50$ and $x_0 = 97668.91$, $\theta = 0.14$, respectively. (For interpretation of the references to color in this figure legend, the reader is referred to the web version of this article.)

for Indian within the next 1.5-2 years by the organization ([Serum Institute initial report on vaccine production](#)). Therefore, a total of 1.5 years from the calculated month of achieving the steady-state (October 2020) is to be taken as the probable time of vaccine development in India.

After having an idea about the probable time of vaccine production, the next step is to predict the implementation time of the vaccine on the entire nation. Literature studies and news releases by the WHO narrate that in case of the smallpox, it took at least 10 years and half a billion vaccine doses in eradicating the disease globally ([smallpox eradication](#)). Using the above mentioned review on the global scenario and the proposed number (1 billion doses) of vaccine production by the Serum Institute of India, we are able to calculate the proposed time of vaccine implementation on total Indian population.

Even if, the rate of immunity gain for the Indian population is also calculated with the help of the percentage decrements of previous smallpox incidence in India from January 1974 to May 1974. The rate of immunity gain can be described as the change in

annual active cases from massive numbers to sudden decrements after applying the vaccine. The case study shows that a total of 187967 people were infected among 68.88 Cr. in 1974. A sudden fall (1436) in the infection was observed in 1975. Moreover, in 1976 the number of active cases further reduced to zero (0) [41]. The application of the vaccine is the obvious reason for such reduction in the active cases ([WHO report](#)).

Finally, we have evaluated the hypothetical incidence and eradication profile for India which are depicted in Fig. 9. Here, we use the estimated value of the parameter of the RGR curve for finding the initial value and asymptotic size of both incidence and eradication profile. The parameters of the hypothetical curves are mentioned in the caption of Fig. 9. The disease eradication rate (r) is estimated as the product of three terms as mentioned earlier. The magnitudes of those three components are 0.00018, 27.8, 3.934 respectively. So by the multiplication of these three values, we get the estimate of r to be 0.019. Thus, the time required to attain the minimum incidence value 50 is approximately 6 years from the calendar date 22/10/2020 which, is no doubt a matter of serious

concern. If we hypothetically assume a pair of eradication rate with 80 % and 90 % lower magnitude, the decreasing disease curves are depicted with red dotted lines. In such cases, the disease can be controlled approximately after 4 and 7 years respectively. We believe that this information is important and can be used as a clue for understanding the eradication process from the management perspectives.

8.4. *r*-strategy and its significance in epidemiology

The bar diagram based on the instantaneous incidence rate (r) of ten countries is exhibited in Fig. 7a. Similar bar diagrams are depicted in Fig. 7b and Fig. 7c for the parameters θ and K , respectively. Here, r is the most important parameter signifies the instantaneous spreading status of the disease of the specific country. We can classify the ten countries based on this high, moderate, and low disease spreading rate. Note that, countries like Mexico, Spain, South Africa, Argentina possess a very high instantaneous incidence rate. These rates are comparatively low for nations like India, Brazil, Colombia, Russia, America, and Peru. A moderate spreading rate is observed for the countries Russia, America, Peru. Judging the overall profile we conclude that, the estimated values of θ are less than 1 for all the countries except Brazil (Figs. 4b–6b). In ecology, the population, which follows the density regulated theta-logistic model with $\theta < 1$ is commonly known as *r*-strategy species. These species can produce many offspring and live in an unstable environment. This concept is synergistic with the epidemiological problem where the disease fitness is initially high with an elevated spreading rate. So, if we assume disease incidence as a population, the SARS-CoV-2 may infect more and more people initially, so that the disease fitness should be increased. The spreading is unpredictable in some sense too as the different countries are associated with the versatile mode of management actions for controlling the disease.

9. Conclusion

The relationship between the corona incidence and its fitness has fundamental implications for the understanding of the corona spreading status of the top ten infected countries. There are significant variations on the corona incidence profiles of the top ten exposed countries. Surprisingly, the incidence-fitness relationship is exhibiting almost a similar trend. This trend is well approximated through the relative growth rate equation of the density regulated theta-logistic model with a concave upward trend. We use a hypothetical time series generated from the estimated RGR profile of the corona incidence and the concept of geometry to predict the population size (*SSIS*) that a plateau or the steady state of COVID-19 will be attained. Our proposed estimate of the time (*SSIT*), at which *SSIS* will be reached, helps in estimating the overall profile of the corona status of different countries. Finally, the *SSIT* value will be useful for taking management decisions and Government policies immediately when a steady state of corona incidence will attain. Moreover, the incremental or detrimental effect of the lockdowns and Unlock phases can also be estimated with the proposed tool of the *SSIT* and *SSIS*.

Funding

The author Ayan Paul is thankful to the Department of Science and Technology, Government of India i.e. DST INSPIRE (Grant Number: IF180793) for supporting the fellowship on such kind of pandemic environment to develop this work. The author Selim Reja is thankful to the University of Grant Commission (UGC), India (Grant Number: 424655) for supporting the fellowship throughout this work.

Declaration of Competing Interest

The authors have no conflict of interest.

CRediT authorship contribution statement

Ayan Paul: Formal analysis, Software, Validation, Visualization, Writing - original draft, Funding acquisition, Methodology, Project administration. **Selim Reja:** Data curation, Software, Validation, Visualization, Funding acquisition. **Sayani Kundu:** Data curation, Validation, Visualization, Methodology. **Sabyasachi Bhattacharya:** Conceptualization, Supervision, Methodology, Project administration.

Acknowledgement

The authors are very much thankful to the final year (4th Semester 2020) M.Stat Students of the Indian Statistical Institute, Kolkata for the initial draft preparation of this manuscript. The literature review sections are developed with the interaction of those students. The authors also thank to the anonymous reviewer for the further modification of the manuscript. The authors must acknowledge to the anonymous reviewer for providing some useful suggestion to improve the quality of the paper.

Supplementary material

Supplementary material associated with this article can be found, in the online version, at [10.1016/j.chaos.2021.110697](https://doi.org/10.1016/j.chaos.2021.110697).

References

- [1] Akaike H. A new look at the statistical model identification. *IEEE Trans Autom Control* 1974;19(6):716–23.
- [2] Alzahran SI, Aljamaan IA, Al-Fakih EA. Forecasting the spread of the COVID-19 pandemic in Saudi Arabia using ARIMA prediction model under current public health interventions. *J Infect Public Health* 2020;13(7):914–19.
- [3] Andrews JM, Langmuir AD. The philosophy of disease eradication. *Am J Public Health Nations Health* 1963;53(1):1–6.
- [4] Aviv E, Aharoni A. Generalized logistic growth modeling of the COVID-19 pandemic in Asia. *Infect Dis Modell* 2020;5.
- [5] Benvenuto D, Giovanetti M, Vassallo L, Angeletti S, Ciccozzi M. Application of the ARIMA model on the COVID-2019 epidemic dataset. *Data Brief* 2020;29:105340.
- [6] Bhattacharya S, Basu A, Bandyopadhyay S. Goodness-of-fit testing for exponential polynomial growth curves. *Commun Stat-Theory Methods* 2008;38(3):340–63.
- [7] Bhattacharya S, Gupta A, Chattopadhyay A. Effect of migration on population growth under dynamical system. *J Appl Probab Stat* 2009;4(2):239–53.
- [8] Bhowmick AR, Bhattacharya S. A new growth curve model for biological growth: some inferential studies on the growth of *Cirrhinus mrigala*. *Math Biosci* 2014;254:28–41.
- [9] Bhowmick AR, Saha B, Chattopadhyay J, Ray S, Bhattacharya S. Cooperation in species: interplay of population regulation and extinction through global population dynamics database. *Ecol Modell* 2015;312:150–65.
- [10] Biswas K, Khaleque A, Sen P. COVID-19 spread: reproduction of data and prediction using a SIR model on Euclidean network. *arXiv preprint arXiv:2003.07063*
- [11] Blumberg A. Logistic growth rate functions. *J Theor Biol* 1968;21(1):42–4.
- [12] Buchanan RL, Cygnarowicz ML. A mathematical approach toward defining and calculating the duration of the lag phase. *Food Microbiol* 1990;7(3):237–40.
- [13] Carlson CJ, Dougherty E, Boots M, Getz W, Ryan SJ. Consensus and conflict among ecological forecasts of Zika virus outbreaks in the United States. *Sci Rep* 2018;8(1):1–15.
- [14] Chakraborty B, Bhattacharya S, Basu A, Bandyopadhyay S, Bhattacharjee A. Goodness-of-fit testing for the Gompertz growth curve model. *Metron* 2014;72(1):45–64.
- [15] Chakraborty B, Bhowmick AR, Chattopadhyay J, Bhattacharya S. Physiological responses of fish under environmental stress and extension of growth (curve) models. *Ecol Modell* 2017;363:172–86.
- [16] Chen T-M, Rui J, Wang Q-P, Zhao Z-Y, Cui J-A, Yin L. A mathematical model for simulating the phase-based transmissibility of a novel coronavirus. *Infect Dis Poverty* 2020;9(1):1–8.
- [17] Chikina M., Pegden W.. Modeling strict age-targeted mitigation strategies for COVID-19. *arXiv preprint arXiv:2004.04144*
- [18] Chimmula VKR, Zhang L. Time series forecasting of COVID-19 transmission in Canada using LSTM networks. *Chaos Solitons Fractals* 2020;135:109864.

- [19] Chowell G, Tariq A, Hyman JM. A novel sub-epidemic modeling framework for short-term forecasting epidemic waves. *BMC Med* 2019;17(1):164.
- [20] Crokidakis N.. Data analysis and modeling of the evolution of COVID-19 in Brazil. *arXiv preprint arXiv:2003.12150*
- [21] Eikenberry SE, Mancuso M, Iboi E, Phan T, Eikenberry K, Kuang Y, et al. To mask or not to mask: modeling the potential for face mask use by the general public to curtail the COVID-19 pandemic. *Infect Dis Modell* 2020;5.
- [22] Fisher RA. Some remarks on the methods formulated in a recent article on "the quantitative analysis of plant growth". *Ann. Appl. Biol.* 1921;7(4):367–72.
- [23] Fokas A, Dikaïos N, Kastis G. Mathematical models and deep learning for predicting the number of individuals reported to be infected with SARS-CoV-2. *J R Soc Interface* 2020;17(169):20200494.
- [24] Forster P, Forster L, Renfrew C, Forster M. Phylogenetic network analysis of SARS-CoV-2 genomes. *Proc Natl Acad Sci* 2020;117(17):9241–3.
- [25] Giordano G, Blanchini F, Bruno R, Colaneri P, Di Filippo A, Di Matteo A, et al. Modelling the COVID-19 epidemic and implementation of population-wide interventions in Italy. *Nat Med* 2020;26:1–6.
- [26] Gompertz B. XXIV. On the nature of the function expressive of the law of human mortality, and on a new mode of determining the value of life contingencies. in a letter to Francis Baily, Esq. *F.R.S. &c. Philos Trans Royal SocLondon* 1825(115):513–83.
- [27] González R.E.. Different scenarios in the dynamics of SARS-CoV-2 infection: an adapted ode model. *arXiv preprint arXiv:2004.01295*
- [28] Gupta A, Bhattacharya S, Chattopadhyay AK. Exploring new models for population prediction in detecting demographic phase change for sparse census data. *Commun Stat-Theory Methods* 2012;41(7):1171–93.
- [29] Gupta R, Pandey G, Chaudhary P, Pal SK. SEIR and regression model based COVID-19 outbreak predictions in India. *medRxiv* 2020.
- [30] Hellewell J, Abbott S, Gimma A, Bosse NI, Jarvis CI, Russell TW, et al. Feasibility of controlling COVID-19 outbreaks by isolation of cases and contacts. *Lancet Global Health* 2020;8.
- [31] Jakhar M, Ahluwalia P, Kumar A. COVID-19 epidemic forecast in different states of india using SIR model. *medRxiv* 2020.
- [32] Kermack WO, McKendrick AG. A contribution to the mathematical theory of epidemics. *Proc R Soc London SerA* 1927;115(772):700–21.
- [33] Khrapov P, Loginova A. Mathematical modelling of the dynamics of the coronavirus COVID-19 epidemic development in China. *Int J Open InfTechnol* 2020;8(4):13–16.
- [34] Krispin R.. Coronavirus: the 2019 Novel coronavirus COVID-19 (2019-nCoV) dataset; 2020. R package version 0.2.0, URL <https://CRAN.R-project.org/package=coronavirus>.
- [35] Kucharski AJ, Russell TW, Diamond C, Liu Y, Edmunds J, Funk S, et al. Early dynamics of transmission and control of COVID-19: a mathematical modelling study. *Lancet Infect Dis* 2020;20:553–8.
- [36] Kucharski AJ, Russell TW, Diamond C, Liu Y, Edmunds J, Funk S, et al. Early dynamics of transmission and control of COVID-19: a mathematical modelling study. *Lancet Infect Dis* 2020.
- [37] Kundu S, Mukherjee J, Yeasmin F, Basu S, Chattopadhyay J, Ray S, et al. Growth profile of *Chaetoceros* sp. and its steady state behaviour with change in initial inoculum size: a modelling approach. *Curr Sci* 2018;115(12):2275.
- [38] Liu T.-H.. A time-dependent sir model for COVID-19 with undetectable infected persons2020;.
- [39] Liu Y, Gayle AA, Wilder-Smith A, Rocklöv J. The reproductive number of COVID-19 is higher compared to SARS coronavirus. *J Travel Med* 2020;27:taaa021.
- [40] Liu Z., Magal P., Seydi O., Webb G.. Predicting the cumulative number of cases for the COVID-19 epidemic in China from early data. *arXiv preprint arXiv:2002.12298*
- [41] Roser M, Ochmann S, Behrens H, Ritchie H, Dadonaite B. Eradication of diseases. *Our World in Data* 2014. <https://ourworldindata.org/eradication-of-diseases>
- [42] Mizumoto K, Chowell G. Transmission potential of the novel coronavirus (COVID-19) onboard the diamond princess cruises ship, 2020. *Infect Dis Modell* 2020;5:264–70.
- [43] Mohamadou Y, Halidou A, Kapen PT. A review of mathematical modeling, artificial intelligence and datasets used in the study, prediction and management of COVID-19. *Appl Intell* 2020;50:3913–25.
- [44] Mukhopadhyay S, Sharma RC, Bhattacharya S, Banik P. Evidences of Allee effect in winter crops: a model based study. *Int J Plant Prod* 2019;14:287–97.
- [45] Nadim SS, Chattopadhyay J. Occurrence of backward bifurcation and prediction of disease transmission with imperfect lockdown: a case study on COVID-19. *Chaos Solitons Fractals* 2020;140:110163.
- [46] Nadim S.S., Ghosh I., Chattopadhyay J.. Short-term predictions and prevention strategies for COVID-2019: a model based study. *arXiv preprint arXiv:2003.08150*
- [47] Pedersen MG, Meneghini M. Quantifying undetected COVID-19 cases and effects of containment measures in Italy. *ResearchGate Preprint* (online 21 March 2020) DOI 2020;10.
- [48] Pelinovsky E, Kurkin A, Kurkina O, Kokoulina M, Epifanova A. Logistic equation and COVID-19. *Chaos Solitons Fractals* 2020;140:110241.
- [49] Peng L., Yang W., Zhang D., Zhuge C., Hong L.. Epidemic analysis of COVID-19 in China by dynamical modeling. *arXiv preprint arXiv:2002.06563*
- [50] Prem K, Liu Y, Russell TW, Kucharski AJ, Eggo RM, Davies N, et al. The effect of control strategies to reduce social mixing on outcomes of the COVID-19 epidemic in Wuhan, China: a modelling study. *Lancet Public Health* 2020;5(5):261–70.
- [51] Prem K, Liu Y, Russell TW, Kucharski AJ, Eggo RM, Davies N, et al. The effect of control strategies to reduce social mixing on outcomes of the COVID-19 epidemic in Wuhan, China: a modelling study. *Lancet Public Health* 2020;5(5):261–70.
- [52] Lin Q, Zhao S, Gao D, Lou Y, Yang S, Musa SS, et al. A conceptual model for the coronavirus disease 2019 (COVID 19) outbreak in Wuhan, China with individual reaction and government action. *Int J Infect Dis* 2020;93:211–16.
- [53] R Core Team. R: a language and environment for statistical computing. Vienna, Austria: R Foundation for Statistical Computing; 2019. URL <https://www.R-project.org/>
- [54] Radulescu A., Cavanagh K.. Management strategies in a SEIR model of COVID 19 community spread. *arXiv preprint arXiv:2003.11150*
- [55] Rahmandad H., Lim T.Y., Sterman J.. Estimating COVID-19 under-reporting across 86 nations: implications for projections and control. Available at SSRN 36350472020;.
- [56] Ranjan R. Predictions for COVID-19 outbreak in india using epidemiological models. *medRxiv* 2020.
- [57] Richards F. A flexible growth function for empirical use. *J Exp Botany* 1959;10(2):290–301.
- [58] Roosa K, Lee Y, Luo R, Kirpich A, Rothenberg R, Hyman J, et al. Real-time forecasts of the COVID-19 epidemic in China from February 5th to February 24th, 2020. *Infect Dis Modell* 2020;5:256–63.
- [59] Saha B, Bhowmick AR, Chattopadhyay J, Bhattacharya S. On the evidence of an Allee effect in herring populations and consequences for population survival: a model-based study. *Ecol Modell* 2013;250:72–80.
- [60] Sandland R, McGilchrist C. Stochastic growth curve analysis. *Biometrics* 1979;35:255–71.
- [61] Sau A, Saha B, Bhattacharya S. An extended stochastic Allee model with harvesting and the risk of extinction of the herring population. *J Theor Biol* 2020;503:110375.
- [62] Seber GAF, Wild CJ. *Nonlinear regression*. 62. Hoboken, New Jersey: John Wiley & Sons; 2003. p. 63.
- [63] Shim E, Tariq A, Choi W, Lee Y, Chowell G. Transmission potential and severity of COVID 19 in South Korea. *Int Soc Infect Dis* 2020.
- [64] Sibly RM, Barker D, Denham MC, Hone J, Pagel M. On the regulation of populations of mammals, birds, fish, and insects. *Science* 2005;309(5734):607–10.
- [65] Singh R., Adhikari R.. Age-structured impact of social distancing on the COVID-19 epidemic in India. 2020arXiv preprint arXiv:2003.12055
- [66] Singh R., Adhikari R.. Age-structured impact of social distancing on the COVID-19 epidemic in India. 2020arXiv preprint arXiv:2003.12055
- [67] Singh RK, Rani M, Bhagavathula AS, Sah R, Rodriguez-Morales AJ, Kalita H, et al. Prediction of the COVID-19 pandemic for the top 15 affected countries: advanced autoregressive integrated moving average (ARIMA) model. *JMIR Public Health and Surveill* 2020;6(2):e19115.
- [68] Song PX, Wang L, Zhou Y, He J, Zhu B, Wang F, et al. An epidemiological forecast model and software assessing interventions on COVID-19 epidemic in China. *medRxiv* 2020.
- [69] Tebbens RJD, Pallansch MA, Cochi SL, Wassilak SG, Linkins J, Sutter RW, et al. Economic analysis of the global polio eradication initiative. *Vaccine* 2010;29(2):334–43.
- [70] Tiwari S, Kumar S, Guleria K. Outbreak trends of coronavirus disease–2019 in India: a prediction. *Disaster Med Public Health Preparedness* 2020;115:1–6.
- [71] Vyasarayani C.P., Chatterjee A.. New approximations, and policy implications, from a delayed dynamic model of a fast pandemic. *arXiv preprint arXiv:2004.03878*
- [72] Wang P, Zheng X, Li J, Zhu B. Prediction of epidemic trends in COVID-19 with logistic model and machine learning technics. *Chaos Solitons Fractals* 2020;139:110058.
- [73] White G, Brisbin I. Estimation and comparison of parameters in stochastic growth models for barn owls.. *Growth* 1980;44(2):97–111.
- [74] Wiecek M, Siłka J, Woźniak M. Neural network powered COVID-19 spread forecasting model. *Chaos Solitons Fractals* 2020;140:110203.
- [75] Zhan C., Tse C., Fu Y., Lai Z., Zhang H.. Modelling and prediction of the 2019 coronavirus disease spreading in China incorporating human migration data. Available at SSRN 35460512020;.
- [76] Zhang H., Guo X., Zeng Y.. Transmissibility of COVID-19 and its association with temperature and humidity2020;.
- [77] Zhang S, Diao M, Yu W, Pei L, Lin Z, Chen D. Estimation of the reproductive number of novel coronavirus (COVID-19) and the probable outbreak size on the diamond princess cruise ship: a data-driven analysis. *Int J Infect Dis* 2020;93:210–4.
- [78] Zhang X, Ma R, Wang L. Predicting turning point, duration and attack rate of COVID-19 outbreaks in major western countries. *Chaos Solitons Fractals* 2020;135:109829.
- [79] Zhao S, Chen H. Modeling the epidemic dynamics and control of COVID-19 outbreak in China. *Quant Biol* 2020;8:11–19.
- [80] Zhao Z, Zhu Y-Z, Xu J-W, Hu Q-Q, Lei Z, Rui J, et al. A mathematical model for estimating the age-specific transmissibility of a novel coronavirus. *medRxiv* 2020.
- [81] Zotin A. Thermodynamics and growth of organisms in ecosystems. *Can Bull Fish Aquat Sci* 1985;213:27–37.